Co(II) and Cu(II) fluorescent complexes with acridine based ligands

Samira Gholizadeh Dogaheh,[a,b] María José Heras Ojea,[a] Lidia Rosado Piquer,[a] Lluís Artús,[a] Hamid Khanmohammadi,[b] Guillem Aromí,[a] E. Carolina Sañudo[a]*

Published as: Eur. J. Inorg. Chem. 2016, 3314–3321

Abstract: The condensation reaction of salicylaldehyde with a diamino organic group (acridine yellow or diaminoacridine) results in the new Schiff base ligands ACRI-1, ACRI-2 and ACRI-3. Fluorescent ACRI-1, ACRI-2 and ACRI-3 have been designed to provide iminophenolic binding pockets for two transition metals and ferromagnetic exchange between the metals. Following our report of $[Co_2(ACRI\text{-}1)_2]$ complex **1Co**, we report here the reactions of ACRI-1, ACRI-2 and ACRI-3 with Co(II) and Cu(II) salts that afford the new fluorescent complexes $[Cu_2(ACRI\text{-}1)_2]$ complex **1Cu,** $[Co_2(ACRI\text{-}2)_2]$ complex **2Co**, $[Cu_2(ACRI\text{-}2)_2]$ complex **2Cu,** $[Co_2(ACRI\text{-}3)_2(H_2O)_4]$ complex **3Co** and $[Cu_2(ACRI\text{-}3)_2]$ complex **3Cu**.

Introduction

The preparation of materials with multiple targeted properties is an important goal in Chemistry, and it poses questions as if synergy between the properties is possible, or if it can be controlled. Our work has always been focused on the study of magnetic properties of coordination complexes. In this area, of particular interest is the synthesis of multifunctional complexes that combine optical and magnetic properties in the same material. The control of the interaction between light and matter is relevant for many fields of technological interest like sensors,[1] bioimaging,[2] photovoltaics[3] for solar energy conversion, light emitting diodes, etc. Many of the materials used are either organic molecules with conjugated groups like the Y123 dye used for dye sensitized solar cells[4] or bulk inorganic materials like the TiO_2 used as anode for solar cells. The development of molecular materials, with all the advantages they have with respect to inorganic bulk materials is an ever growing hot-topic: molecular materials can be prepared at room temperature in solution and are soluble in common organic solvents.[5] In particular we are interested in coordination complexes, where the properties are a combination of the properties of the metal (catalysis, magnetism, emission properties,...) and the properties of the ligand (fluorescence, surface grafting ability,...). In coordination complexes properties can be tuned by designed functionalization of the ligands, during the synthesis step. One example is the synthesis of coordination complexes with thiol substituted ligands for grafting on gold electrodes and surfaces.[6],[7] This brings us to a key point for the development of single-molecular devices or devices using molecular species: scientists need to be able to design multifunctional molecules that can be grafted on surfaces in a controlled and ordered manner [6,8,9] in order to prepare devices and finally allow addressing single molecules.[6],[10],[11]

The combination of a fluorescent ligand with a transition metal gives rise to a photosensitive response that is affected by coordination, and thus excellent chemosensors have been reported exploiting particular effects such as metal coordination induced excimer, or metal coordination induced emission shift. With respect to the intensity of the emission, the coordination of transition metals to a fluorescent group gives rise to two general optical effects: transition metals with unpaired electrons usually provoke a quenching of the fluorescence (chelation enhancement of quenching, CHEQ effect) while metals without unpaired electrons like Zn(II) provoke an enhancement of the fluorescent signal (chelation enhancement of fluorescence, CHEF effect). The combination of magnetic properties with fluorescence is not straight forward, due to the CHEQ effect. However some have succeeded in the preparation of coordination complexes with specially designed ligands that combine fluorescence ligands and SMM properties,[12–14] and fluorescence and ferromagnetism.[15] In this respect, ligand design is very important in order to obtain multifunctional, optical and magnetic complexes, as the emission properties of the ligand can be easily quenched by metal coordination. The optical properties can also be envisioned as a switch for the magnetic properties, and this field poses many challenges but also promises many technological applications. Matsuda and co-workers, among others have succeeded in using nitronylnitroxide radicals combined with a central diarylethene photochromic unit to exploit magnetic and optical properties in the same species without transition metals. They showed how the photoswitching of the diradical interaction can be controlled

[a] ECS, MJHO,LA, LRP, GA
Departament de Química Inorgànica i Institut de Nanociència i Nanotecnologia, Universitat de Barcelona. Av. Diagonal 645, Barcelona, 08028, SPAIN
E-mail: esanudo@ub.edu
Homepage: http:// www.gmmf-ub.com
[b] SGD,HK
Department of Chemistry, Faculty of Science, Arak University, Arak 38156-8-8349, Iran

Supporting information for this article is given via a link at the end of the document.

by a photochromic ring opening/closing reaction.[16] The diarylethene basic unit can also be exploited as ligand to transition and lanthanide metals. Yamashita and co-workers have exploited the photochromic open/close reaction of a functionalized dithienyl-ethene compound as ligand for Dy(III) to affect the quantum tunnelling properties of the compound[17] and to link Mn_4 SMMs into 1D chains.[18] We chose the strongly luminescent group acridine yellow, and its analogue diaminoacridine as the central part of the bidentate ligands ACRI-1, ACRI-2 and ACRI-3, shown in Scheme 1. The ligands are the Schiff base obtained form condensation of the diamine central fluorescent moiety with an aldehyde. The relative disposition of the two binding pockets should result in ferromagnetic coupling between two metals coordinated to one ligand.[19],[20] We have shown how the ACRI-1 Co(II) complex $[Co_2(ACRI\text{-}1)_2]$ **1Co** was a robust fluorescent ferromagnet that could be deposited intact on HOPG.[15] For the surface deposition, the ligand was designed with aromatic rings that would help pi-pi stacking and Van der Waals interactions with the graphite surface. The ACRI-x ligands have anthracene-like cores, selected due to their optical properties. The anthracene derivatives and other polyaromatic units have been shown to display pairwise packing emission with lifetimes that become longer proportional to the degree of overlapping of two facing anthracene π-planes,[21] as well as providing access to non-linear-optics (NLO) systems when combined with diarylenes.[22] In this paper we report new Cu(II) complex of ACRI-1 and Cu(II) and Co(II) ACRI-2 and ACRI-3 complexes. All the paramagnetic species display weak to ferromagnetic coupling when changing the metal from Cu(II) to Co(II). All the paramagnetic complexes show fluorescent emission red shifted from the free ligand.

Results and Discussion

Following our report of the Schiff base ligand ACRI-1 we report here the synthesis of the analogous new fluorescent ligands ACRI-2 and ACRI-3 shown in Scheme 1. ACRI-2 is the Schiff base obtained by the condensation reaction between diaminoacridine hydrochloride and two equivalents of salicylaldehyde. ACRI-3 differs with ACRI-1 in the naphtyl-OH groups instead of the phenol groups and for its synthesis 2-hydroxy-naphtaldehyde is used instead of salicylaldehyde.

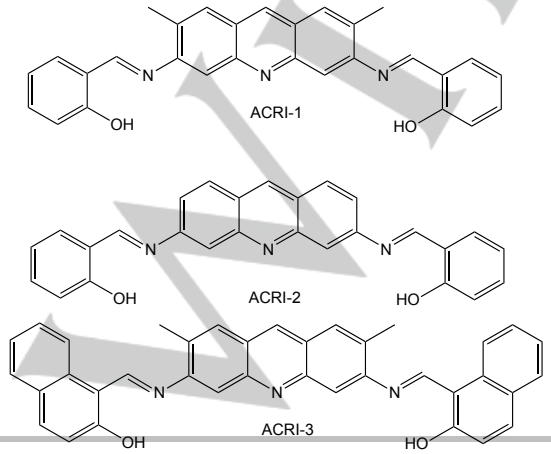

Scheme 1. Chemdraw structures of the acridine Schiff base ligands.

The ligands were obtained in good yield and characterized by IR, MS and proton NMR. As we reported in 2014, the reaction of the ligand ACRI-1 with a cobalt(II) salt resulted in a precipitate which was recrystallized and characterized as $[Co_2(ACRI\text{-}1)_2]$ (**1Co**).[15] In complex **1Co** the two cobalt ions are tetracoordinated in a distorted tetrahedral environment. Following the same synthetic procedure we report here the preparation of the new fluorescent complexes $[Cu_2(ACRI\text{-}1)_2]$ (**1Cu**), $[Co_2(ACRI\text{-}2)_2]$ (**2Co**), $[Cu_2(ACRI\text{-}2)_2]$ (**2Cu**), $[Co_2(ACRI\text{-}3)_2(H_2O)_4]$ (**3Co**) and $[Cu_2(ACRI\text{-}3)_2]$ (**3Cu**). The reaction of the metal salt with the ligand in the presence of base results in a precipitate. The yield of precipitate is very good in all cases and IR comparison of the precipitates with the crystalline products obtained after recrystallization show without ambiguities that they are the same material. The reactions with ACRI-2 were performed in MeCN following the synthesis of complex **1Co**. However, ACRI-3 contains naphtyl groups and it is markedly less soluble than ACRI-1 and ACRI-2, so reactions in MeCN lead to poor yields due to undisolved ligand. The ligand is more soluble in dmf and reactions in this solvent lead to acceptable yields. We have not been able to obtain crystal suitable for single-crystal X-ray diffraction for the Co(II) complexes of ACRI-2 (complex **2Co**) and ACRI-3 (complex **3Co**), however these species can be characterized by paramagnetic proton NMR and compared to the spectrum of complex **1Co**. Following the typical pattern observed for Co(II) complexes the proton NMR spectra of complexes **2Co** and complex **3Co** show chemical shifts between 70 and -50 ppm. The observed paramagnetic shifts are in agreement with the values reported in the literature for other Co(II) complexes.[23] The proton NMR of complex **2Co** is analogous to the reported for complex **1Co** confirming that the reaction of hydrated $Co(NO_3)_2$ with ACRI-2 produces $[Co_2(ACRI\text{-}2)_2]$ (**2Co**).

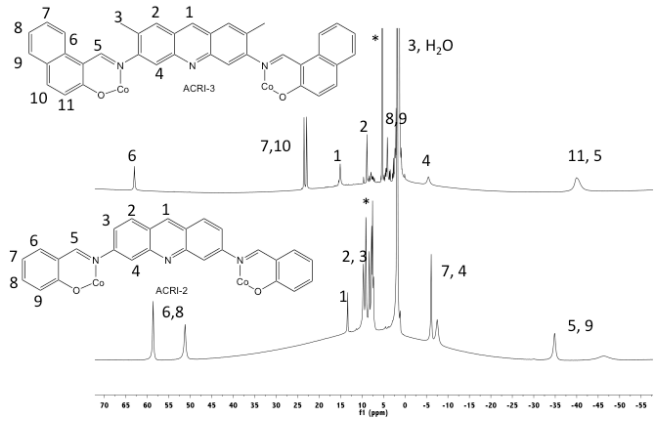

Figure 1. Proton NMR of the paramagnetic complexes $[Co_2(ACRI\text{-}2)_2]$ **2Co** (in $CDCl_3$) and complex $[Co_2(ACRI\text{-}3)_2(H_2O)_4]$ **3Co** (in CD_2Cl_2).

The proton NMR for complex **3Co** is what one would expect if the phenyl group is replaced by a naphtyl group which confirms the formation of $[Co_2(ACRI\text{-}3)_2(H_2O)_4]$, (**3Co**). A broad peak overlaps with the methyl signal (protons assigned number 3 in the Figure 1) and this could be due to water coordinated to the cobalt, which also appears in the elemental analysis of dried samples of complex **3Co**.

The proton NMR of the Cu(II) complexes **1Cu, 2Cu** and **3Cu** show very broad signals due to the fast relaxation at room temperature of protons of an organic ligand bound to Cu(II) with S = 1/2. The proton NMR does not provide useful structural information. Fortunately we were able to obtain suitable crystals for single-crystal X-Ray diffraction of these species.

Description of crystal structures

Crystallographic and data collection information for complexes **1Cu**, **2Cu** and **3Cu** can be found in Table 1. The crystal structure of complex **1Cu** was collected at two different temperatures (100 K and 296 K) and the two structures showed the same asymmetric units and $CHCl_3$ solvent molecules. The dinuclear complex is practically isostructural for the three species, the main differences being related to the distortion from ideal geometry of the coordination environment of the metal. Figure 2 shows the dinuclear unit in **1Cu**, **2Cu** and **3Cu**. For complex **2Cu**, the asymmetric unit contains two independent half dinuclear units, as was the case for complex **1Co.** For **1Cu** and **3Cu** the asymmetric unit contains only 1/2 dinuclear unit with solvent molecules. First let's describe the dinuclear unit $[M_2(ACRI\text{-}X)_2]$ common to the three complexes. Complex **1Cu** contains ACRI-1, complex **2Cu** contains ACRI-2, which has protons instead of the methyl groups of ACRI-1 and complex **3Cu** contains ACRI-3, with naphtol units instead of phenol.

Table 1. Crystallographic and data collection parameters for complexes **1Cu**·$8CHCl_3$, **2Cu**·$5CHCl_3$ and **3Cu**·4dmf.

	1Cu·$8CHCl_3$	**2Cu**·$5CHCl_3$	**3Cu**·4dmf
T/K	100(2)	100(2)	100(2)
Crystal system	triclinic	triclinic	monoclinic
Space group	P-1	P-1	$P2_1/c$
a/Å	10.9946(10)	12.1838(10)	12.390(3)
b/Å	13.4255(12)	15.2799(13)	8.1305(16)
c/Å	15.0453(15)	17.2458(14)	35.406(7)
α/°	110.219(5)	90.463(6)	90.00
β/°	106.823(5)	95.775(6)	90.468(3)
γ/°	94.432(6)	105.264(6)	90.00
V/Å^3	1955.5(3)	3079.6(4)	3566.5(12)
Z	1	2	2
Radiation	MoKα	MoKα	MoKα
Gof on F^2	1.074	1.065	0.893
Final R indexes [I>=2σ (I)]	R_1 = 0.1033, wR_2 = 0.2624	R_1 = 0.0774, wR_2 = 0.2004	R_1 = 0.0515, wR_2 = 0.1375
Final R indexes [all data]	R_1 = 0.1304, wR_2 = 0.2768	R_1 = 0.1296, wR_2 = 0.2392	R_1 = 0.0741 wR_2 = 0.1573

Each metal ion is tetracoordinated to two nitrogen and two oxygen donors, from two iminophenolic/iminonaphtolic binding pockets from two ACRI-X ligands. The two ligands bridge the metals and display intra-molecular π-π stacking between the acridine cores with distances around 3.4 Å. A close examination of the structural parameters (see Table 2) clearly shows that the tetracoordinated metal centre is distorted from the ideal tetrahedral or square planar coordination. The Co(II) complex **1Co** is the closer to an ideal tetrahedral coordination environment while the Cu(II) complexes are closer to distorted square-planar coordination, which results in 'flatter' molecules.

Even though the dinuclear unit is quite similar, the supramolecular organization of the $[M_2(ACRI\text{-}X)_2]$ units is very different. The crystal packing of complex **1Cu**·$8CHCl_3$ is shown in Figure 3, the crystal structure was collected at 296 K and at 100 K and the packing and crystallographic parameters are the same for both temperatures. In complex **1Cu**·$8CHCl_3$ the dinuclear units form a supramolecular structure of empty hexagonal channels along the *a* axis of the unit cell by π-π stacking of the phenolic aromatic groups, with phenyl-phenyl distances of 3.6 Å. These channels are partially filled with eight chloroform molecules per complex and leave clear pores along the crystal of 0.5 nm of diameter. The chloroform molecules are localized and held in place by Cl_3C-H···N interactions at 3.3 Å and Cl···H-C interaction at distances between 3.8 and 4.2 Å with aromatic C-H bonds from the phenolic[24] and central acridine groups. Upon exposure to heat or vacuum most of the chloroform molecules are lost and the supramolecular structure collapses, as shown by elemental analyses and the powder X-ray diffraction data (see Supplementary Information, Figure S3). The chloroform-**1Cu** interaction is not selective. Recrystallization of complex **1Cu** from 1:10 mixtures of $CHCl_3$:CH_2Cl_2 and $CHCl_3$:dmf resulted in **1Cu**·$4CH_2Cl_2$ and **1Cu**·4dmf (see supplementary information Table S1 and Figures S2 and S3), the crystal structures are not porous.

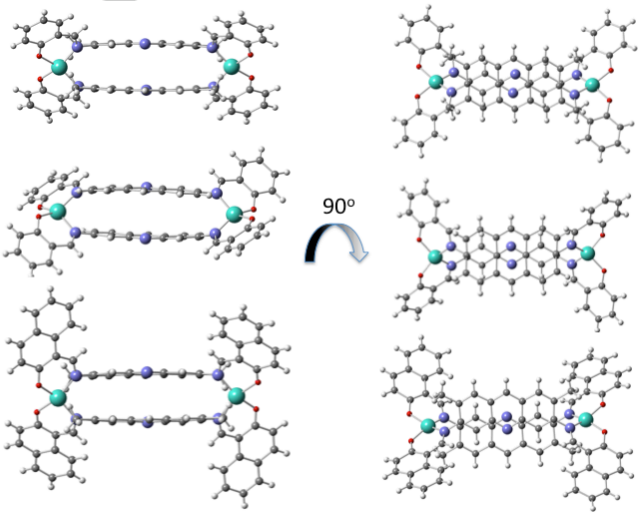

Figure 2. Two views of the crystal structure of complex **1Cu** (top), **2Cu** (middle) and **3Cu** (bottom). Copper, cyan; oxygen, red; nitrogen, light blue, carbon, grey; hydrogen: light grey. (Colour online).

Crystals of **1Cu**·$4CH_2Cl_2$ and **1Cu**·4dmf were exposed to vapours of chloroform in order to see if the solvent was replaced by chloroform since solvent replacement in single-crystal to single-crystal transformations are known but uncommon.[25] However, in this case the single crystals were destroyed and the chloroform did not replace CH_2Cl_2 or dmf in the structure. From

the data in Table 2 and the packing of complexes **1Cu**·8CHCl$_3$, **2Cu**·5CHCl$_3$ and complex **1Co** in CHCl$_3$[15] one can conclude that the packing is dictated by the coordination sphere of the metal but this is not the only factor. With distorted square planar Cu(II) a porous structure is formed with the ligand ACRI-1 in **1Cu**·8CHCl$_3$, however, when the methyls are removed in **2Cu**·5CHCl$_3$, or the phenyl group is replaced by a naphtyl like in **3Cu**·4dmf the Cu(II) complex is not as flat as complex **1Cu** (clearly seen in Figure 2) and it crystallizes in a compact structure similar to that reported for complex **1Co.**

Table 2. Structural details of **1Co**, **1Cu**, **2Cu** and **3Cu**. The ideal value for the average L-M-L angle is 109º for a ideal tetrahedral geometry and 90º for ideal square planar, The ideal value for the torsion NN-OO is 90º for a ideal tetrahedral geometry and 0º for ideal square planar. For complexes **1Co** and **2Cu** there are two symmetry independent molecules.

	1Co·4CHCl$_3$ (ref 15)	**1Cu**·8CHCl$_3$	**2Cu**·5CHCl$_3$	**3Cu**·4dmf
M-M (Å)	12.01 11.90	12.24	12.12 12.18	12.01
(ACRI) N-N (Å)	3.19, 3.26	3.36	3.639 3.454	3.409
O-M-O (o)	107.09 113.86	86.58	97.90, 89.85	86.37
O-M-N (o)	95.78, 95.71 96.46, 95.42	93.13, 93.27	93.22, 93.18 93.78, 93.27	91.16, 91.48
N-M-N (o)	105.12 108.41	96.42	99.16 99.93	101.07
Average L-M-L (o)	100.9 103.5	92.35	95.8 94.2	92.52
Torsion NN-OO (o)	57.51 55.38	34.35	38.97 47.36	32.14

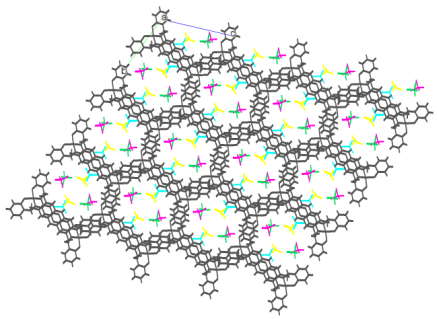

Figure 3. Crystal packing of **1Cu**·8CHCl$_3$, the molecules are colored by symmetry equivalence, complex **1Cu** in gray and CHCl$_3$ molecules in pink, yellow, green and blue.

Magnetic properties

The dc magnetic susceptibility of complex **1Co** showed that it is a ferromagnet with T_C = 5 K, as reported in 2014.[15] We studied the dc magnetic susceptibility of complexes **1Cu**, **2Co, 2Cu, 3Co** and **3Cu** in the 2-300 K temperature range and at applied dc fields of 300 Oe and 5000 Oe. The data are shown in Figure 4 and Figure 5 as χT vs. T plots. The magnetic behaviour of complex **2Co** is analogous to the reported for **1Co**. For complex **2Co**, the χT product at 300 K is in agreement with two Co(II) ions in tetrahedral environment (S = 3/2 and g = 2.0). As temperature decreases the χT product is nearly constant until a sharp increase is observed at 50 K. At this temperature the two fields diverge. Below 10 K the χT product drops dramatically due to magnetic anisotropy. The ac magnetic susceptibility data show the appearance of a frequency independent peak at 5 K and the ZFC/FC data, shown in Figure S4, show a divergence at 5 K. Unfortunately, crystals of complexes **2Co** and **3Co** have not been obtained. With the information of the proton NMR can assume a similar solid state structure as that of **1Co**, with similar intermolecular interactions to rationalize the ordering observed in the ac data. The magnetic data for complex **3Co** shows a χT product value at 300 K that is more in agreement with two hexacoordinated Co(II) ions with spin-orbit coupling than the expected for two tetrahedral Co(II). As T decreases the χT product decreases, as is typical for Co(II) with strong spin-orbit coupling. According to the magnetic data the Co(II) ions in **3Co** are hexacoordinated. This is in agreement with the elemental analyses performed on oven-dried samples, which show the presence of coordinated water.

For complexes **1Cu**, **2Cu** and **3Cu** the χT product at 300 K is in agreement with two isolated Cu(II) ions with S = 1/2 and g = 2.0. As temperature decreases the χT product is nearly constant until a very small increase takes place at very low temperatures, in agreement with two Cu(II) ions with very weak ferromagnetic coupling. The magnetic data for the Cu(II) complexes can be modelled with the software PHI.[26] PHI is a computer package that uses the phenomenological Hamiltonian $\hat{H} = \hat{H}(Crystal\ Field) + \hat{H}(Zeeman) - 2J_{ij}\sum \hat{S}_i \cdot \hat{S}_j$. This system is solved by evaluating the matrix elements of the Hamiltonian over the basis states and diagonalizing the Hamiltonian matrix. Two simulations using only the exchange and Zeeman Hamiltonians for a ferromagnetically coupled dimer of S = 1/2 are shown in Figures 5 as solid lines. The parameters for the simulations of the susceptibility data were g = 2.0 and a very weak exchange of J = 0.2 cm^{-1} (red line) or J = 0.8 cm^{-1} (blue line). The simulation with J = 0.2 cm^{-1} is closer to the experimental data for complexes **1Cu** and **2Cu**, while the

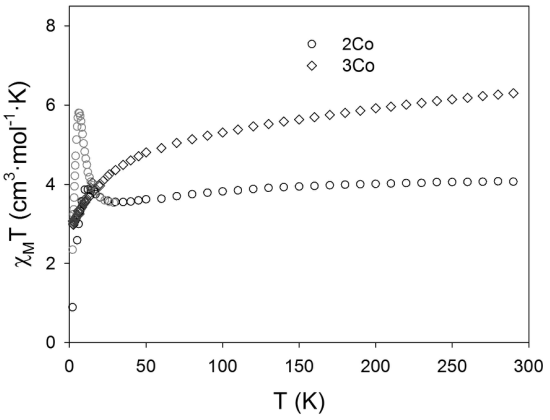

Figure 4. Magnetic susceptibility data for complexes **2Co** (circles) and **3Co** (squares) shown as χT vs. T plots measured at 0.5 T and 300 Oe (below 30 K).

simulation with J = 0.8 cm^{-1} fits better the experimental data for complex **3Cu**. The two metals are *circa* 1.2 nm apart in these

dinuclear complexes. Still, magnetic coupling (even though very weak for Cu(II)) is observed.

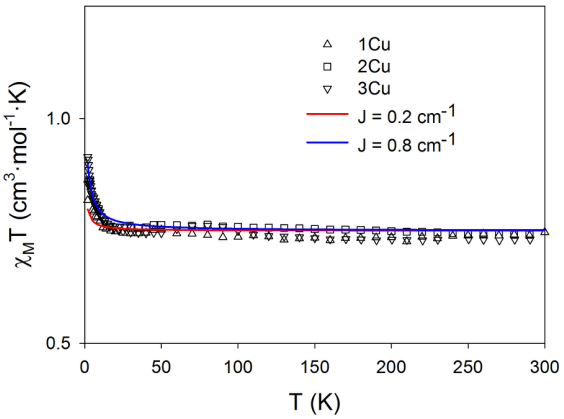

Figure 5. Magnetic susceptibility data for complex **1Cu** (triangles), **2Cu** (squares) and **3Cu** (triangles down) shown as χT vs. T plots measured at 0.3 T. The solid lines are simulations, see text for parameters.

A spin polarization mechanism as that observed in the proton NMR of complexes **2Co** and **3Co** explains the stabilization of the high spin states for the Co(II) and Cu(II) complexes. The magnetization vs. field data collected at 2 K are shown in Figure 6. As expected due to the very small exchange constant calculated by DFT for **1Co** and using PHI software for **1Cu**, **2Cu** and **3Cu** the excited states lie close in energy to the ground state and this is reflected in the magnetization vs. field curves, even at 2 K, due to Boltzman population of the excited states. The crystal field Hamiltonian was used along with a giant spin model for S = 1 to simulate the magnetization data. The crystal field parameters were $B_2^0\theta_2$ = |0.7| and |0.5| cm^{-1} for the two simulations. This calculation does not take into account the exchange between the two Cu(II) ions. There is no evidence of long-range order for the Cu(II) complexes **1Cu**, **2Cu** and **3Cu** down to 2 K.

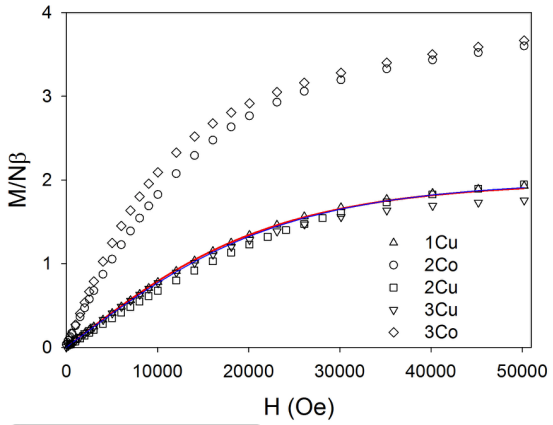

Figure 6. Magnetization vs. field plots for complexes **2Co** (circles), **1Cu** (triangles), **2Cu** (squares), **3Co** (diamonds) and **3Cu** (triangles down) at 2 K. The solid lines are simulations, see text for parameters.

Fluorescent properties

All emission spectra were collected in chloroform solutions of the ligand or complexes. Figures 7-9 show the emission spectra of the new ligands ACRI-2, ACRI-3 and the Co and Cu complexes. The electronic and emission spectra of the new ligand ACRI-2 are very similar to those previously reported for ACRI-1.[15,27] The electronic and emission spectra of ACRI-3 show the additional band from the naphtyl groups. In particular, this is seen as two maxima in the emission spectra.

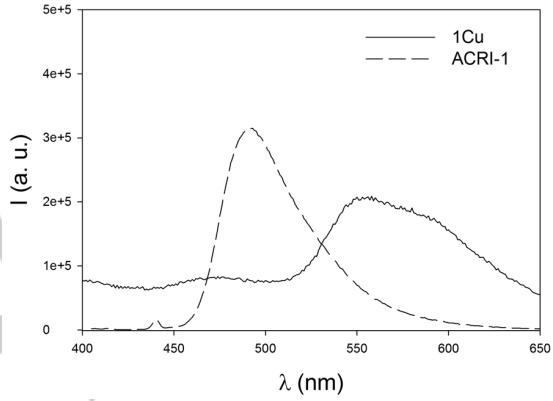

Figure 7. Emission vs. wavelength plots for the ligand ACRI-1 (1e-6 M) and complex **1Cu** (1e-3 M) at an irradiation wavelength of 350 nm.

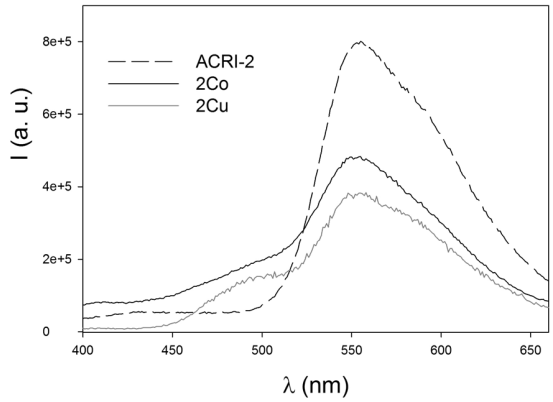

Figure 8. Emission spectra of ACRI-2 (1e-6 M, Ix0.8) in chloroform and the complexes **2Co** (1e-6 M) in dichloromethane and **2Cu** (1e-6 M, Ix2) in chloroform at an irradiation wavelength of 350 nm.

The electronic spectra of the free ligands ACRI-2 and ACRI-3 were studied in $CHCl_3$ and CH_2Cl_2 solution (see supplementary material). Broad intense absorption bands expected for an organic compound with phenyl/naphtyl, imine and anthracene

groups were observed between 475 and 240 nm. The electronic spectra of the cobalt and copper complexes show the typical absorption bands of the aromatic ligand and the very weak d-d transitions from Co(II) or Cu(II).

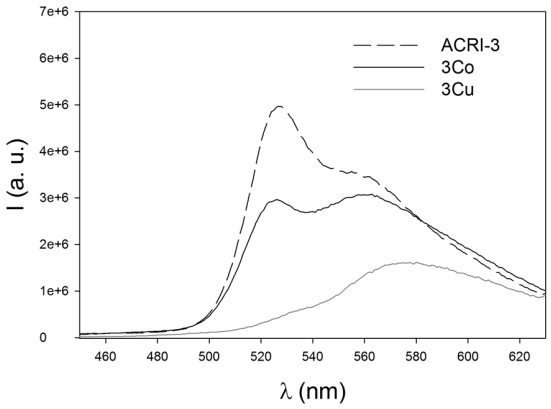

Figure 9. Emission spectra of ACRI-3 (1e-6 M) and complexes **3Co** and **3Cu** (1e-6 M) at irradiation wavelength of 320 nm.

The wavelengths of 350 nm and 320 nm were chosen to irradiate the samples and study the emission spectra, as they are assigned to ligand-centred absorption processes. When a 10^{-6} M solution of ACRI-2 is irradiated at wavelengths between 350 and 400 nm an emission band at 550 nm is observed, shown in Figure 8. At lower concentrations this band shifts to 490 nm. Intermolecular interactions in concentrated solutions facilitate relaxation pathways of lower energy, probably *via* excimer formation. However, even at such low concentrations as 10^{-9} M it is impossible to observe the fluorescence of the purely isolated acridine core of the ligand ACRI-2, which should appear around 450 nm and show vibronic fine structure, as observed for ACRI-1[15] and usual for anthracene derivatives.[28]

Irradiation of 10^{-6} M samples of complexes **1Cu**, **2Co** and **2Cu** in $CHCl_3$ at 350 nm results in fluorescent emission bands from the ligand around 550 nm, as shown in Figures 7 and 8. The emission spectra of complex **2Cu** [Cu_2(ACRI-2)$_2$] was scaled by a factor of 2 in order to observe the band clearly, since at similar concentration the emission band was less intense than for the other complexes. This effect has previously been seen with curcuminoid-copper complexes, where a spin-driven quenching mechanism is invoked.[29] Coordination of the paramagnetic metals Co(II) and Cu(II) does not result in a complete quench of the fluorescence of the ligand. All the complexes present emission bands shifted to lower energies from the free ligand, this is easily explained by the intramolecular π-π stacking interaction between the acridine cores (see N-N distance in Table 2), observed clearly in the solid state crystal structure, which is retained in solution if the molecule does not dissociate. This intramolecular interaction has a similar effect to excimer formation, providing additional pathways for relaxation at lower energies.

Emission spectra for ACRI-3 were collected on 10^{-6} to 10^{-9} M solutions of the ligand in CH_2Cl_2. The sample was irradiated at a wavelength of 320 nm. The spectrum is shown in Figure 9. Clearly two emission bands are observed, at 530 and 580 nm. The highest energy band is assigned to the naphtyl groups while the 580 nm band is assigned to the acridinefluorofore. When the ligand ACRI-3 is coordinated to Co(II) or Cu(II) a quenching of the fluorescence is observed. The emission spectra of complexes **3Co** and **3Cu** are shown in Figure 9. Solution of the complexes at 10^{-6} M were prepared in CH_2Cl_2 and irradiated at 320 nm. As we observed for the ACRI-1 and ACRI-2 complexes, the quenching of the fluorescent emission is more pronounced for the Cu(II) complex. In both spectra one can observe the two emission bands, assigned to the naphtyl and acridine fluorofores.

Conclusions

Rational ligand design of ACRI-1, ACRI-2 and ACRI-3 allows access to ferromagnetically coupled, fluorescent complexes of Co(II) and Cu(II). Reaction of the ligands with Co(II) and Cu(II) have afforded the new fluorescent complexes [Cu_2(ACRI-1)$_2$] complex **1Cu**, [Co_2(ACRI-2)$_2$] complex **2Co**, [Cu_2(ACRI-2)$_2$] complex **2Cu**, [Co_2(ACRI-3)$_2$] complex **3Co** and [Cu_2(ACRI-3)$_2$] complex **3Cu**. All complexes display ferromagnetic coupling between the metal centres. Complex [Co_2(ACRI-2)$_2$] **2Co**, like the ACRI-1 analogue, displays supramolecular ferromagnetic interactions. Using the same crystallization solvent, the preference for square planar or tetrahedral coordination of the metal determines the shape of the [M_2(ACRI-X)$_2$] moiety, which is reflected in compact packing for [Co_2(ACRI-1)$_2$] (**1Co**) with distorted tetrahedral Co(II) and a porous structure for [Cu_2(ACRI-1)$_2$] complex **1Cu** with distorted square planar Cu(II). **1Cu**·8$CHCl_3$ retains $CHCl_3$ in the channels at room temperature and these chloroform molecules are lost in a non-reversible process upon exposure to heat or vacuum. The reported complexes are exciting new examples of fluorescent magnetic materials, where the two properties co-exist and can be triggered separately. For further studies on the control of the magnetic properties of a nanoscale magnetic system using light,[30] the complexes reported here can be deposited on carbon based materials like graphene and carbon nanotubes, as we previously have done for complex **1Co.** The optical properties of the ligand are retained in the coordination complex. This opens up exciting possibilities in which one can envision using the emission of the acridine-based ligands for switching on/off magnetic exchange or even quantum tunnelling and slow relaxation.

Experimental Section

All chemicals were purchased from commercial sources and used as received. The ligand ACRI-1 was prepared following the reported procedure.[15]

$C_{27}H_{19}N_3O_2$·HCl (ACRI-2). To a mixture of 3,6-diaminoacridine hydrochloride ($C_{13}H_{12}N_3Cl$) (2 g, 8.14 mmol) and triethylamine (5.7 mL, 40.70 mmol) in ethanol (100 mL) was added salicyladehyde (1.7 mL, 16.28mmol). The resulting solution was stirred and heated up to 79 ºC. Reflux was maintained during eight hours. After standing overnight, a precipitate is filtered, washed with ethanol and dried with diethyl ether. The yield of the reaction is 89% (3.29 g obtained). The ligand was characterized by ^{1}H NMR, EA and ESI-MS. MW($C_{27}H_{19}N_3O_2$) = 417 g/mol. Ms/z ($M+1H^+$)= 418.16.Elemental Anal. Calc. of $C_{27}H_{19}N_3O_2$·HCl: C, 71.50; H, 4.45; N, 9.27. Experimental: C, 70.82; H, 4.45; N, 9.54%.

$C_{37}H_{27}N_3O_2$·HCl (ACRI-3). To a mixture of Acridine Yellow hydrochloride ($C_{15}H_{16}N_3Cl$) (1.218 g, 4.45mmol) and triethylamine (3.099 mL, 29mmol) in ethanol (100 mL) was added 2-hydroxy-naphtaldehyde (1.532 g, 8.89 mmol) in 20 mL of EtOH. The resulting solution was stirred and heated up to 79 ºC. Reflux was maintained for seven hours. After standing overnight, a precipitate is filtered, washed with ethanol and dried with diethyl ether. The yield of the reaction is 82% (2.01 g obtained). The ligand was characterized by ^{1}H NMR, IR and ESI-MS. MW($C_{37}H_{27}N_3O_2$)= 545.21 g/mol. Ms/z ($M+1H^+$)= 546.22.

[Cu_2(ACRI-1)$_2$] (1Cu). A solution of the ligand ACRI-1 ($C_{29}H_{23}N_3O_2$) (0.147 g, 0.31mmol) in acetonitrile (20 mL) was treated with $CuCl_2$·H_2O (0.051 g, 0.31 mmol) and three equivalents of Et_3N (128 μL, 0.92 mmol). The color of the solution changes from orange to brownish green. A precipitate is filtered after 24 h stirring, washed with acetonitrile, and dried with diethyl ether. Yield 89% (0.135 g). Slow evaporation of a chloroform solution of the precipitate results in the formation of single crystals of [Cu_2(ACRI-1)$_2$]·8$CHCl_3$ (**1Cu**). ESI-MS: MW = 1012 Ms/z ($M+H^+$) = 1013. Elemental Anal. Calc. of [Cu_2(ACRI-1)$_2$]·3.2($CHCl_3$): C 52.85; H 3.27; N 6.04. Experimental: C, 52.89; H, 3.42; N, 6.07%. Selected IR data in cm^{-1} (KBr): 3420.57 (w), 3012.42 (w), 1606.63 (s), 1582.86 (s), 1529.01 (s), 1456.06 (s), 1435.40 (s), 1377.65 (m), 1326.20 (m), 1187.94 (w), 1150.78 (w), 1132.66 (m), 1033.25 (w), 998.42 (w), 913.39 (w), 869.11 (w), 757.56 (w), 742.26 (w), 667.75 (w), 636.75 (w), 574.14 (w), 494.99 (w).

[Co_2(ACRI-2)$_2$] (**2Co**). A solution of the ligand ACRI-2 (0.156 g, 0.34 mmol) in acetonitrile (20 mL) was treated with $Co(NO_3)_2$·$6H_2O$ (0.100 g, 0.34 mmol) and three equivalents of Et_3N (144 μL, 1.03 mmol). The color of the solution changes from ochre to dark brown. After 24 hours of stirring a precipitate is filtered, washed with acetonitrile, and dried with diethyl ether. Yield 82% (0.134 g). Slow evaporation of a chloroform solution of the precipitate results in the formation of crystals of [Co_2(ACRI-2)$_2$] (**2Co**). The compound was characterized by ^{1}H NMR. ESI-MS: MW = 948 g/mol. Ms/z ($M+1H^+$) = 949. Elemental Anal. Calc. of [Co_2(ACRI-2)$_2$]·1.75($CHCl_3$): C 57.94; H 3.12; N 7.27. Experimental: C, 58.00; H, 3.50; N, 7.00%. Selected IR data in cm^{-1} (KBr): 3375.76 (w), 1604.03 (s), 1574.59 (s), 1525.82 (s), 1506.47 (w), 1486.66 (w), 1431.52 (s), 1383.83 (s), 1317.44 (w), 1248.33 (w), 1172.32 (w), 1147.59 (s), 975.02 (w), 910.67 (w), 876.79 (w), 863.56 (w), 809.51 (w), 772.96 (w), 754.50 (w), 634.24 (w).

[Cu_2(ACRI-2)$_2$] (**2Cu**). A solution of the ligand ACRI-2 (0.266 g, 0.58 mmol) in acetonitrile (20 mL) was treated with $CuCl_2$·H_2O (0.100 g, 0.59 mmol) and three equivalents of Et_3N (245 μL, 1.76 mmol). The color of the solution changes from ochre to reddish brown. After 2 hours of stirring a precipitate is filtered, washed with acetonitrile, and dried with diethyl ether. Yield 86% (0.254 g). Slow evaporation of a chloroform solution of the precipitate results in the formation of single crystals of [Cu_2(ACRI-2)$_2$]·5$CHCl_3$ (**2Cu**). ESI-MS: MW = 956Ms/z ($M+H^+$) = 957. Elemental Anal. Calc. of [Cu_2(ACRI-2)$_2$]·1.5($CHCl_3$): C 58.78; H 3.15; N 7.41. Experimental: C, 58.22; H, 3.85; N, 7.70%. Selection of the IR data in cm^{-1} (KBr): 3365.16 (w), 1605.33 (s), 1585.02 (s), 1530.48 (s), 1448.67 (s), 1386.12 (m), 1321.85 (m), 1173.29 (s), 1147.35 (s), 988.92 (w), 911.04 (w), 871.59 (w), 815.13 (w), 756.19 (w), 667.68 (w), 572.69 (w), 526.20 (w).

[Co_2(ACRI-3)$_2$(H_2O)$_4$] (**3Co**). A solution of the ligand **ACRI-3** (0.320 g, 0.587 mmol) in dmf (20 mL) was treated with $Co(NO_3)_2$·$6H_2O$ (0.17 g, 0.58 mmol) and three equivalents of Et_3N (245μL, 1.76 mmol). The color of the solution changes from ochre to dark brown. After 24 hours of stirring a precipitate is filtered, washed and dried with diethyl ether. Yield 81% (0.286 g). The compound was characterized by ^{1}H NMR.ESI-MS: MW = 1204 g/mol. Ms/z ($M+1H^+$-4(H_2O))= 1205. Elemental Anal. Calc. of [Co_2(ACRI-3)$_2$(H_2O)$_4$]·2(H_2O): C 67.66; H 4.76; N 6.40. Experimental: C, 67.71; H, 3.93; N, 6.60 %. Selected IR data in cm^{-1} (KBr): 3421(s), 1599(s), 1569(w), 1535(s), 1465(w), 1384(s), 1358(w), 1302(w), 1186(w), 1132(w), 1007(w), 832(w), 746(w).

[Cu_2(ACRI-3)$_2$] (**3Cu**). A solution of the ligand **ACRI-3** (0.320 g, 0.58 mmol) in dmf (20 mL) was treated with $CuCl_2$·$2H_2O$ (0.10 g, 0.58 mmol) and three equivalents of Et_3N (245 μL, 1.76 mmol). The color of the solution changes from ochre to brown. After 24 hours of stirring a precipitate is filtered, washed and dried with diethyl ether. Yield 21.62% (0.077 g). Slow diethyl ether diffusion on the mother liquor results in the formation of crystals of [Cu_2(ACRI-3)$_2$] (**3Cu**). ESI-MS: MW = 1214.32 g/mol. Ms/z ($M+1H^+$) = 1216.5. Elemental Anal. Calc. of [Cu_2(ACRI-3)$_2$]·: C 73.19; H 4.15; N 6.92. Experimental: C, 73.40; H, 4.27; N, 6.88%. Selected IR data in cm^{-1} (KBr): 3396(w), 1615(s), 1600(s), 1572(s), 1536(s), 1452(w), 1428(w), 1384(w), 1365(w), 1306(w), 1188(w), 1133(w), 831(w), 748(w).

Experimental techniques

Single crystal diffraction data for all the compounds were collected on a Bruker APEXII SMART diffractometer at the Facultat de Química, Universitat de Barcelona, using a 30 microfocus Molybdenum kα radiation source. The structures were solved by direct methods (SHELXS97) and refined on F2 (SHELX-97). Cif files can be obtained free of charge form the Cambridge Crystallographic Data Centre (CCDC https://summary.ccdc.cam.ac.uk/structure-summary-form, deposit codes: **1Cu**·8$CHCl_3$: 1416991, 1416992; **1Cu**·4CH_2Cl_2: 1416994; **1Cu**·4dmf: 14169995; **2Cu**·5$CHCl_3$: 1416994; **3Cu**·dmf: 1474844). Hydrogen atoms were included on calculated positions, riding on their carrier atoms. Infra-Red spectra were performed on a Thermo scientific AVATAR 330 FT-IR; Fluorescence measures were taken in a NanoLogTM-Horiba JobinYvon iHR320 spectrophotometer; UV-Vis spectra were acquired in a Cary 100 Scan from Varian. Elemental analyses were carried out at the CCiT-UB and CSIC. Magnetic measurements on crushed polycrystalline, vacuum dried samples (SQUID magnetometer equipped with a 5T magnet, diamagnetic correction applied using Pascal's constants) were done at the Servei de Mesures Magnètiques of CCiT-UB.^{1}H-NMR (Varian Unity 300 MHz on manual mode) were performed at the NMR service of CCiT-UB.

Acknowledgements

ECS, MJHO, LA, LRP, GA acknowledge financial support from the Spanish Government via FEDER Funding (CTQ 2012/32247). LA acknowledges to UB the opportunity to work at GMMF for his Final Year Project (Treball de Fi de Grau). SG acknowledges support from Iranian Ministry of Science Research and Technology (MSRT) for funding for a stay at GMMF-UB.

Keywords: coordination chemistry • multifunctional • magnetic properties • fluorescence

[1] Z. Liu, W. He, Z. Guo, *Chem. Soc. Rev.* **2013**, *42*, 1568–600.

[2] A. J. Amoroso, S. J. A. Pope, *Chem. Soc. Rev.* **2015**, *44*, 4723–4742.

[3] G. Bottari, G. de la Torre, D. M. Guldi, T. Torres, *Chem. Rev.* **2010**, *110*, 6768–6816.

[4] J.-H. Yum, E. Baranoff, F. Kessler, T. Moehl, S. Ahmad, T. Bessho, A. Marchioro, E. Ghadiri, J.-E. Moser, C. Yi, et al., *Nat. Commun.* **2012**, *3*, 631–639.

[5] I.-R. Jeon, R. Clérac, *Dalton Trans.* **2012**, *41*, 9569–86.

[6] D. Gatteschi, A. Cornia, M. Mannini, R. Sessoli, *Inorg. Chem.* **2009**, *48*, 3408–3419.

[7] A. Ghirri, V. Corradini, V. Bellini, R. Biagi, U. del Pennino, V. De Renzi, J. C. Cezar, C. A. Muryn, G. A. Timco, R. E. P. Winpenny, et al., *ACS Nano* **2011**, *5*, 7090–9.

[8] M. Mannini, D. Bonacchi, L. Zobbi, F. M. Piras, E. A. Speets, A. Caneschi, A. Cornia, A. Magnani, B. J. Ravoo, D. N. Reinhoudt, et al., **2005**, *12*, 4–7.

[9] A. Pons-balagué, S. Piligkos, S. J. Teat, J. Sánchez Costa, M. Shiddiq, S. Hill, G. R. Castro, P. Ferrer-Escorihuela, E. C. Sañudo, *Chem. Eur. J.* **2013**, *19*, 9064–9071.

[10] A. Candini, S. Klyatskaya, M. Ruben, W. Wernsdorfer, M. Affronte, *Nano Lett.* **2011**, *11*, 2634–2639.

[11] L. Bogani, W. Wernsdorfer, *Nat. Mater.* **2008**, *7*, 179–186.

[12] M. Menelaou, F. Ouharrou, L. Rodríguez, O. Roubeau, S. J. Teat, N. Aliaga-Alcalde, *Chemistry* **2012**, *18*, 11545–11549.

[13] M. Pacchioni, A. Cornia, A. C. Fabretti, L. Zobbi, D. Bonacchi, A. Caneschi, G. Chastanet, D. Gatteschi, R. Sessoli, *Chem. Commun. (Camb).* **2004**, *2*, 2604–5.

[14] T. N. Nguyen, K. a. Abboud, G. Christou, *Polyhedron* **2013**, *66*, 171–178.

[15] M. J. Heras Ojea, D. Reta Mañeru, L. Rosado, J. Rubio Zuazo, G. R. Castro, S. Tewary, G. Rajaraman, G. Aromí, E. Jiménez, E. C. Sañudo, *Chem. - A Eur. J.* **2014**, *20*, 10439–10445.

[16] K. Matsuda, M. Irie, *Chem. - A Eur. J.* **2001**, *7*, 3466–3473.

[17] G. Cosquer, M. Morimoto, M. Irie, A. Fetoh, B. K. Breedlove, M. Yamashita, *Dalt. Trans.* **2015**, *44*, 5996–6002.

[18] M. Morimoto, H. Miyasaka, M. Yamashita, M. Irie, *J. Am. Chem. Soc.* **2009**, *131*, 9823–9835.

[19] R. H. Laye, E. C. Sañudo, *Inorganica Chim. Acta* **2009**, *362*, 2205–2212.

[20] T. Glaser, M. Heidemeier, S. Grimme, E. Bill, *Inorg. Chem.* **2004**, *43*, 5192–5194.

[21] S. Hisamatsu, H. Masu, M. Takahashi, K. Kishikawa, S. Kohmoto, *Cryst. Growth Des.* **2015**, *15*, 2291–2302.

[22] K. Okuno, Y. Shigeta, R. Kishi, M. Nakano, *J. Phys. Chem. Lett.* **2013**, *4*, 2418–2422.

[23] E. C. Sañudo, T. B. Faust, C. A. Muryn, R. G. Pritchard, G. A. Timco, R. E. P. Winpenny, *Inorg. Chem.* **2009**, *48*, 9811–9818.

[24] A. Mukherjee, S. Tothadi, G. R. Desiraju, *Acc. Chem. Res.* **2014**, *47*, 2514–2524.

[25] J. S. Costa, S. Rodríguez-Jiménez, G. a Craig, B. Barth, C. M. Beavers, S. J. Teat, G. Aromí, *J. Am. Chem. Soc.* **2014**, *136*, 3869–74.

[26] N. F. Chilton, R. P. Anderson, L. D. Turner, A. Soncini, K. S. Murray, *J. Comput. Chem.* **2013**, *34*, 1164–1175.

[27] D. Reta Mañeru, M. J. Heras Ojea, L. Rosado, G. Aromí, J. A. Zuazo, G. R. Castro, E. C. Sañudo, *Polyhedron* **2013**, *66*, 136–141.

[28] T. Seko, K. Ogura, Y. Kawakami, H. Sugino, H. Toyotama, J. Tanaka, *Chem. Phys. Lett.* **1998**, *291*, 438–444.

[29] N. Aliaga-Alcalde, L. Rodríguez, M. Ferbinteanu, P. Höfer, T. Weyhermüller, *Inorg. Chem.* **2012**, *51*, 864–873.

[30] A. Nurbawono, C. Zhang, *Appl. Phys. Lett.* **2013**, *103*, 0–4.

Entry for the Table of Contents (Please choose one layout)

FULL PAPER

Magnetic and optical materials are in the spotlight, where one can envision using light to switch the magnetic properties. This is relevant to fields as diverse as information storage, processing or molecular spintronics. In this paper the authors report the synthesis and characterization of new multifunctional magnetic and fluorescent complexes with a ligand based on the acridine group.

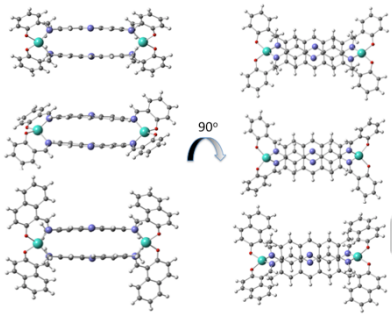

Multifunctional complexes: fluorescent and magnetic

*Samira Gholizadeh Dogaheh, María José Heras Ojea, Lidia Rosado Piquer, Lluís Artús, Hamid Khanmohammadi, Guillem Aromí, E. Carolina Sañudo**

Page No. – Page No.

Co(II) and Cu(II) fluorescent complexes with acridine based ligands